Rapidity distribution in two-chain model of soft hadronic interactions

Tadeusz Wibig and Dorota Sobczyńska
Experimental Physics Department, University of Łódź, Nowotki 149/153, 90-236 Łódź, Poland
(Received 1 June 1992)

The data on proton-nucleus interactions measured in 1982 at the CERN SPS were parametrized within the multichain model. Since that time very accurate new measurements have been made by the EHS-NA22 Collaboration, which require a more accurate new description of multiparticle production processes. In this paper we do this parametrization for the rapidity distributions of meson (π^+ and K^+) and proton interactions with protons at the laboratory momentum of 250 GeV/c. We examine the self-consistency of the two-chain model of soft hadronic interactions and extrapolate it to the hadron-nucleus and nucleus-nucleus collisions. The comparison of the model predictions with the data is presented and satisfactory agreement between the data and our parametrization at $\sqrt{s} \sim 20$ GeV is achieved.

PACS number(s): 13.85.Hd, 12.40.Aa, 12.40.Lk, 25.40.Ve

I. INTRODUCTION

The two-chain multiparticle production model of soft hadronic interactions at low energies is based on the general idea of the dual parton model (DPM) [1] established well in theoretical terms; however, it is not in conceptual contradiction with the other models such as the Lund, multifireball, geometrical, or additive quark model (AQM) [2]. All of them can provide similar results in the energy region well known experimentally [below energies reached at the CERN Intersecting Storage Rings (ISR)], in which soft interactions play a dominant role.

In this paper we would like to show, on the basis of rapidity distribution, that the two-chain mechanism of low energy hadronic interactions allows for a natural extension of the hadron-hadron interaction picture to hadron-nucleus and nucleus-nucleus collisions. The description of such processes is quite similar to that proposed by the AQM. There are some improvements against this model which are natural and lead to a better description of the data. On the other hand, the proposed procedure is not as complicated as in the DPM or FRITIOF models and can be used to develop Monte Carlo codes of much faster soft interaction generators, which is important in some cases, e.g., in extensive air shower simulation programs in cosmic ray physics.

The DPM picture of p-N interactions [3] is given in Fig. 1. The particle production is going through two chains (1 and 2 in Fig. 2) produced in the first interaction of incoming proton and through the subsequent pairs of chains (3 and 4) from each following interaction inside the nucleus. The first two are similar to those presented in Fig. 2(a), where the DPM mechanism of the soft p-p interaction [1] is shown. The first approximation assumed in this paper is that rapidity distributions of the particles produced from chain decays are exactly the same. The shapes of rapidity distributions from other chains (3 and 4) can, of course, be different, but some of their characteristics can be taken from the experimental data on meson-proton collision. The data available presently contain well-measured rapidity distributions of meson interactions. The DPM picture of meson-proton collision is shown in Fig. 2(b). The difference between Figs. 2(a) and 2(b) is, in general, only in one end of the chain marked by 2. For the interaction of protons this chain end is formed by the diquark, while in the meson-proton interaction by one valence quark only. Thus we can expect the difference in rapidity distributions of the produced particles in the forward direction between proton and meson induced interactions. It is clearly seen in the experimental data. When trying to find the shapes of rapidity distributions of the products of chains 3 and 4 in Fig. 1 we have noticed that DPM pictures of those chains are very similar to those in Fig. 2(b). We have assumed that the shapes of rapidity distributions of the products

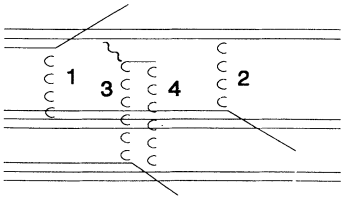

FIG. 1. DPM picture of soft proton-nucleus interaction.

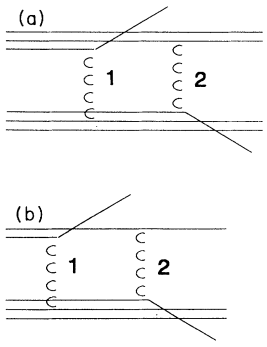

FIG. 2. Two-chain DPM picture of (a) a proton-proton interaction and (b) a meson-proton interaction.

of sea-quark ends of the chains (3 and 4) are the same as for valence-quark ends in the meson-induced interaction chains. Because of the overlapping of rapidity distributions coming from different chains in the region where the sea-quark ends of chains give a contribution to the measured rapidity distribution this assumption cannot be verified by comparing with experimental data. On the other hand, it means that the results of our fitting procedure are not very sensitive to the details of the fragmentation of sea-quark ends of the chains. The final agreement with the data obtained in the present paper justifies somehow all simplifying assumptions we have made.

II. PARAMETRIZATION OF THE RAPIDITY DISTRIBUTION IN THE TWO-CHAIN PICTURE OF HADRON-PROTON INTERACTIONS

The data on the rapidity distribution of the hadron (π^+,K^+,p) interaction with protons at the laboratory momentum of 250 GeV/c are available for negative and positive particles separately. It allows us to study the effect of "leading particle" on the shape of the rapidity distributions as well as to estimate the probability of charge exchange of the incoming particle.

First we examine negative particle distributions, which are not disturbed by charge exchange. As has been said the negative particle distribution is the sum of two distributions produced from two chains [Fig. 2(b)]. Our parametrization distinguishes between strange and nonstrange chains. Because of the high accuracy of the experimental data the small discrepancy between kaon- and pion-induced interactions in the forward hemisphere rapidity distributions is seen. As is discussed in Ref. [4] this is due to the fact that there is a strange quark in the kaon, for which the fragmentation can be a little different than for nonstrange quarks. This can be seen in our parametrization.

The fitting procedure used for π^- rapidity distributions gives a very accurate fit to the tails of the distribution which can be described by Gaussians. To reproduce all the distributions as a sum of two distributions with the fitted Gaussian tails it is necessary to introduce a relatively flat plateau describing the particle production in the central parts of fragmenting chains. The distribution fitted to fragmentation products of each chain is of the form

$$\frac{1}{N}\left[\frac{dn}{dy}\right]_i = \begin{cases} A_i \exp\left[-\dfrac{(y-y_B)^2}{2\sigma_B^2}\right], & y \le y_B, \\ A_i, \quad y_B \le y \le y_F, \\ A_i \exp\left[-\dfrac{(y-y_F)^2}{2\sigma_F^2}\right], & y_F \le y, \end{cases} \tag{1}$$

where the number of particles formed from the chain i is equal to

$$\langle n_i \rangle = A_i \left[(y_F - y_B) + \left[\frac{\pi}{2}\right]^{1/2} (\sigma_B + \sigma_F)\right] . \tag{2}$$

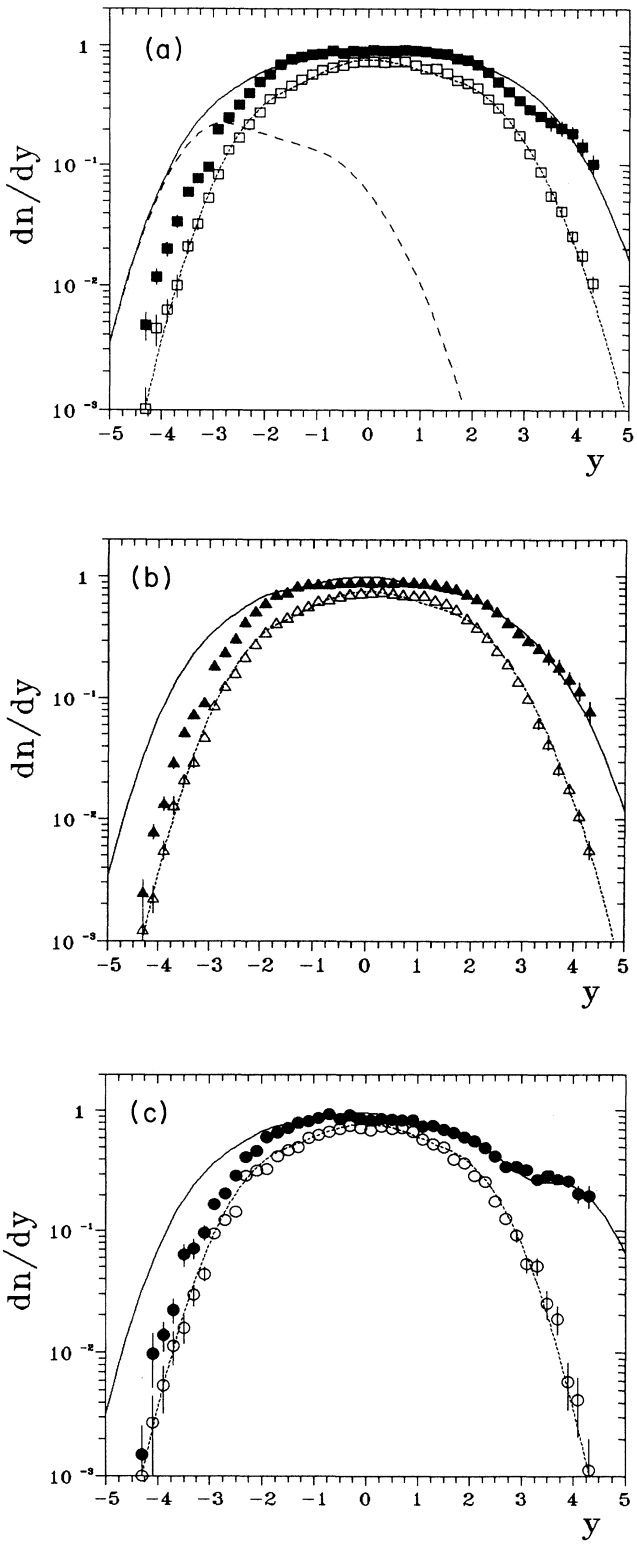

FIG. 3. Rapidity distributions of negatively (open symbols and short dashed lines) and positively (solid symbols and solid lines) charged particle for (a) π^+-p, (b) K^+-p, and (c) p-p interactions at 250 GeV/c compared with our two-chain parametrization predictions. The backward-leading proton distribution is shown in (a) by the long dashed line.

We have found that the positions of the inner ends of each chain (y_B for forward and y_F for backward chains, respectively) can be fixed at a center-of-mass rapidity 0. The results of our fits are shown in Fig. 3 with the data taken from Ref. [4]. For the p-p interaction we assume for both outer tails the diquark end fragmentation and for the inner tails the same as for a meson-induced interaction distribution of quark end fragmentation products. The parameters of the fit are listed in Table I.

The next step is to examine positive particle distributions, which consist of the following.

(i) The baryons: if we neglect baryon pair production inside the fragmenting chain, we expect baryons to be leading particles only. Some of them are protons and some, due to the process called "change exchange," are neutrons, which are not observed in the experiment.

(ii) The leading mesons, which carry the excess charge from recharged leading baryons.

(iii) The bulk of the produced particles come from the same mechanism as the negative pions for which we assume the same rapidity distribution as for those described above.

In the EHS-NA22 experiment slow protons (with $p_{\text{lab}} < 1.2$ GeV/c) are identified and excluded from the data, but the charge excess still exists in both forward and backward hemispheres. An additional extra positive charge is about 1.6 (mean multiplicity of slow protons [5] is ~ 0.34 for π^+-p interactions) and is carried by leading protons and extra positive pions. The charge exchange probability is assumed to be equal to $\frac{1}{3}$. The shapes of the rapidity distributions of additional mesons are calculated from the rapidity distributions of the chains fitted to the π^- distributions in the following way:

$$N_{\text{ex}}(y) \sim \exp\left[-\int_{\substack{\text{end of}\\ \text{the chain}}}^{y} N_i(y') \frac{dy'}{\Delta} \right], \tag{3}$$

where the parameter Δ equals 1. It is consistent with the assumption that the charge exchange takes place between a leading particle and the most energetic neutral pion. The integral of N_{ex} over the whole rapidity range is normalized to the mean multiplicity of charge-exchanged leading particles.

The baryons listed in (i) contribute to the rapidity distribution of positive particles within the range of large rapidity values. At this stage of the fitting procedure it is not possible to calculate them directly as carrying the rest of the incoming momentum; so their rapidity distributions are fitted to the data. The integral over the whole rapidity range of the charged baryon distribution together with the leading charged meson distribution (ii) should equal 1 (charge of the chain induced by the incoming particle). It has been found that the shapes of those distributions within error limits are identical to those of excess pions (ii) but shifted to higher (lower for the backward chain) rapidities. Two parameters describing those shifts are introduced and their values equal ~ 1.0 (~ 2.0 for forward leading protons). For forward leading protons it should be noticed (cf. Ref. [6]) that in the experiment all particle masses are taken as a pion mass. This leads to the shift in the rapidity of protons with high rapidities (if they are misidentified). This shift is about 1; so in our fitting procedure the leading mesons and protons have approximately the same mechanisms of creating their rapidities.

The accuracy of our fits of rapidity distributions of positive particles can be seen in Fig. 3. The discrepancy in the backward hemisphere is due to the low-energy protons excluded from the experimental data. The rapidity distribution of backward leading protons is shown as a dashed line in the figure. All the parameters of the fit are listed in Table I.

III. PARAMETRIZATION OF THE HADRON-NUCLEUS INTERACTION

To describe rapidity distributions in hadron-nucleus collisions it is necessary to calculate probabilities of the number of hadron collisions inside a target nucleus. We proceed this by a simple geometrical approach. For the distribution of nuclei in the nucleus we use a well-known

TABLE I. Parameters for the parametrization of hadron-proton interactions at the laboratory momentum of 250 GeV/c.

	π^+-p	K^+-p	p-p
Forward chain	$\sigma_F = 0.95$	$\sigma_F = 0.95$	$\sigma_F = 0.80$
	$\sigma_B = 0.95$	$\sigma_B = 0.95$	$\sigma_B = 0.95$
	$y_F = 1.60$	$y_F = 1.50$	$y_F = 1.55$
	$y_B = 0$	$y_B = 0$	$y_B = 0$
	$\langle n \rangle = 1.80$	$\langle n \rangle = 1.70$	$\langle n \rangle = 1.45$
Backward chain	$\sigma_F = 0.95$	$\sigma_F = 0.95$	$\sigma_F = 0.95$
	$\sigma_B = 0.80$	$\sigma_B = 0.80$	$\sigma_B = 0.80$
	$y_F = 0$	$y_F = 0$	$y_F = 0$
	$y_B = -1.60$	$y_B = -1.60$	$y_B = -1.55$
	$\langle n \rangle = 1.20$	$\langle n \rangle = 1.20$	$\langle n \rangle = 1.45$
Excess π^+	$\Delta = 1.$	$\Delta = 1.$	$\Delta = 1.$
	$\langle n_{\text{ex}} \rangle = 1/3$	$\langle n_{\text{ex}} \rangle = 1/3$	$\langle n_{\text{ex}} = 1/3$
Leading particle	$Y_{\text{shift } B} = -1.$	$Y_{\text{shift } B} = -1.$	$Y_{\text{shift } B} = -1.$
	$Y_{\text{shift } F} = 1.$	$Y_{\text{shift } F} = 1.$	$Y_{\text{shift } F} = 2.$
	$\langle n_{\text{lead}} \rangle = 1 - \langle n_{\text{ex}} \rangle$	$\langle n_{\text{lead}} \rangle = 1 - \langle n_{\text{ex}} \rangle$	$\langle n_{\text{lead}} \rangle = 1 - \langle n_{\text{ex}} \rangle$

formula

$$\rho(R)=\begin{cases}\dfrac{A}{(a\sqrt{\pi})^3}\exp\left[-\left[\dfrac{R}{a}\right]^2\right] & \text{for } A<40,\\ \dfrac{\rho_0}{1+\exp[(R-c)4.4/t]} & \text{for } A\geq 40,\end{cases} \tag{4}$$

which is Gaussian and of Fermi type for lighter and heavier nuclei, respectively.

The parameters of that formula are fitted to describe data on a total inelastic cross section. The values used in the present paper are

$$\begin{aligned} a&=(1.5)^{-1/3}R_{\rm rms}\ ,\\ R_{\rm rms}&=1.18A^{1/3}\ ,\\ c&=1.128A^{1/3}\ ,\\ t&=2.5\ [\text{fm}]\ . \end{aligned} \tag{5}$$

In Table II we present the calculated values of probabilities of the given numbers of π^+ and K^+ interactions inside the target nuclei of Al and Au, obtained by Monte Carlo calculations.

As has been pointed above, the particle production in the hadron interaction with the nucleus can be treated as a composition of decaying chains. For the negative particle production we can introduce (i) the backward chain from the first interaction (No. 1 in Fig. 1), (ii) the backward chain from the second interaction inside the nucleus (No. 4 in Fig. 1), (iii) the backward chain from the ith interaction, (iv) the forward chain (No. 2 in Fig. 1), (v) the extra recharged backward chain from the first interaction, (vi) the extra recharged backward chain from the second interaction, (vii) the extra recharged backward chain from the ith interaction, (viii) the additional chain from the second interaction (No. 3 in Fig. 1), and (ix) the additional chain from the ith interaction.

The final negative rapidity distribution for the interaction with a fixed number of interactions inside the target nucleus is the sum of all the contributions. A mean rapidity distribution is the sum of distributions with the fixed number of interactions weighed by the probabilities of each number of interactions calculated in the way presented above.

TABLE II. Probabilities of the multiple interaction of the hadron inside a nucleus.

No. of interactions	Probabilities of a given number of interactions $\nu\pi^+$ Al	K^+ Al	π^+ Au	K^+ Au
1	0.63	0.69	0.32	0.35
2	0.23	0.21	0.22	0.25
3	0.10	0.07	0.18	0.18
4	0.03	0.02	0.13	0.11
5	0.01	0	0.08	0.06
6	0		0.05	0.03
7			0.02	0.01
8			0.01	0
$\langle\nu\rangle$	1.55	1.47	2.65	2.33

We assume that the backward and forward chain rapidity distributions are the same as for the interaction with a proton. The backward chains for the second and other subsequent interactions in the nucleus are shifted in reference to the previous one by the value of ΔY_N. This can be understood as a result of energy losses of the forward-going chain. In general, its value can be calculated by making an assumption about the transverse momentum distribution and its correlations with particle rapidity.

The forward chain for the hadron-nucleus interaction with a fixed number of interactions inside the nucleus (ν_i) is assumed to be shifted as well but its shift equals ($\nu_i\Delta Y_N$).

The extra negatives are introduced here as the products of recharging the neutron from the target nucleus. Their spectra are calculated in the same way as the spectra of the products of recharging the proton to π^+ in the hadron-proton interaction described by (3). For the charge exchange probability we adopt here the value of $\frac{1}{3}$ as well.

The rapidity distribution of additional chain products [(viii) and (ix)] cannot be taken directly from the parametrization of the hadron-proton interactions presented. Its shape should be like in (1), and we also assume that it is symmetrical in the c.m. system (c.m.s.) ($y_B=-y_F$ and $\sigma_B=\sigma_F$). The value of σ_B equals the value of quark fragmentation end of the chain calculated above.

Rapidity distributions of additional chain products are shifted backward subsequently by the ΔY_N.

In addition to the component listed above for the positive particle spectra we have to introduce the following: (x) forward-leading particle; (xi) extra recharged forward particles; (xii) backward-leading particles from each interaction inside the target.

We get their spectra exactly from the fit to the hadron-proton interaction. For the first two we introduce the shift ($\nu_i\Delta Y_N$) in the same way as for forward chain products.

The accuracy of the reproduction of the data for 250 GeV/c from Ref. [7] is presented in Fig. 4. Additional parameters are listed in Table III.

To check our fits with the data on proton-nucleus collisions we use the data from Ref. [8] at the laboratory energy of 200 GeV/nucleon measured at Fermilab.

The change of incoming proton energy leads only to the change of lengths of plateau in our chain parametrization from 1.55 at 250 GeV/c to 1.5 at 200 GeV/c. All other parameters remain unchanged.

The comparison of the data for p-p, p-Mg, p-Ag, and p-Au with our fits is given in Fig. 5. No significant systematic discrepancies are observed. The overestimation

TABLE III. Parameters of the rapidity distribution of additional chain products.

Additional chain	$\sigma_F=0.95$
	$\sigma_B=0.95$
(from the second interaction inside the	$y_F=1.5$
target nucleus)	$y_B=-1.5$
	$\langle n_{\rm add}\rangle=0.6$
$\Delta Y_N=-0.2$	

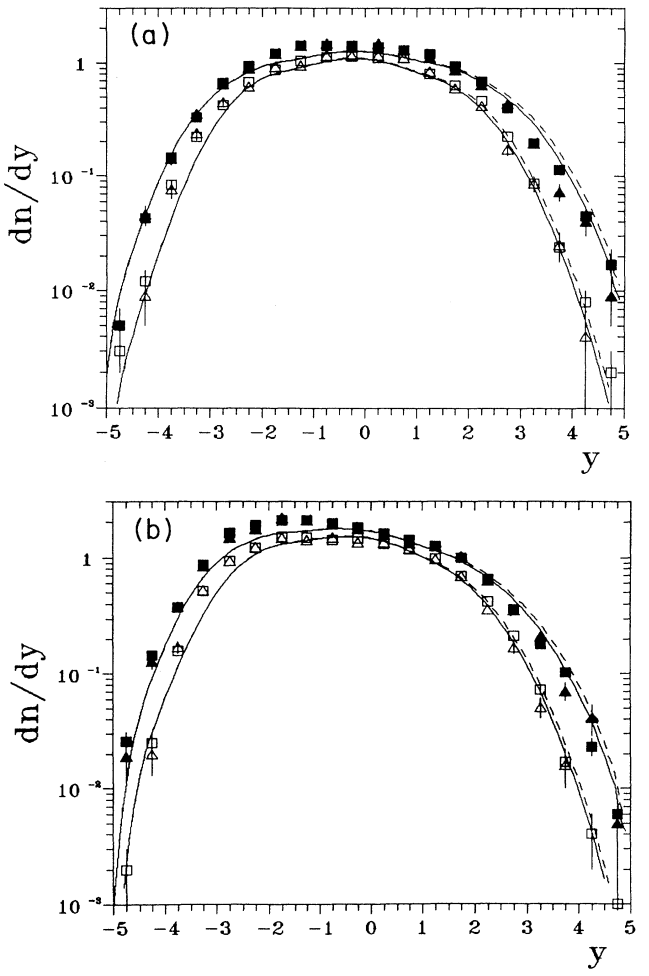

FIG. 4. Measured rapidity distributions of positively (solid symbols) and negatively (open symbols) charged particles for (a) π^+-Al (squares), K^+-Al (triangles) and (b) π^+-Au (squares), K^+-Au (triangles) interactions at 250 GeV/c in comparison with our two-chain parametrization predictions (dashed line for π^+- and solid for K^+-induced interactions, respectively).

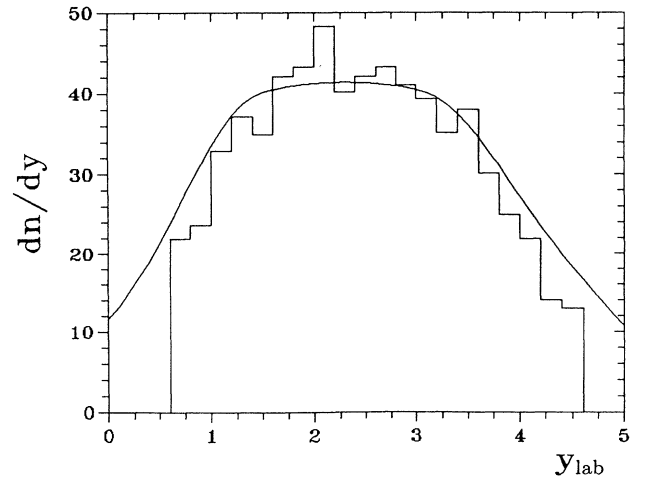

FIG. 5. Rapidity distributions of all charged particles for proton interactions with different targets (p, Mg, Ag, and Au) at 200 GeV/c (curves) compared with the experimental data.

seen in an extremely backward region can be removed by a small narrowing of the additional chain product distribution with ν. This will, among others, be discussed in the next section.

IV. PARAMETRIZATION OF THE NUCLEUS-NUCLEUS RAPIDITY DISTRIBUTION

We extend our fitting procedure to nucleus-nucleus interactions. The DPM description of such processes leads to the conclusion that they are a composition of four different types of internal interactions: namely [9], (i) interactions between pairs of nucleons (one from each nucleus), (ii) second and subsequent interactions of the wounded nucleon from the beam nucleus with the nucleon from the target, (iii) interactions of nucleons from the beam with the wounded nucleons from the target, and (iv) interactions between wounded nucleons.

The first (i) type of interactions is assumed to be similar to the first interaction in the nucleon-nucleus interaction picture producing both forward and backward chains, as has been described for the forward chain in such interactions.

The second (ii) and the third (iii) types are symmetrical with respect to beam-target exchange. They can, in general, be treated in the same way as the second and each following interaction in the nucleon-nucleus interaction described in the previous section.

The fourth (iv) types of interactions should give a relatively small amount of produced particles even in comparison with the events of type (iii). Thus we neglect them and the results confirm this statement.

The extension of the above presented fitting procedure to nucleus-nucleus collisions does not introduce any free parameters to be fitted to the data. All those used by us are fitted to the hadron-hadron interaction and those obtained for the additional chain to the products in the hadron-nucleus data.

To calculate the probabilities of the numbers of in-

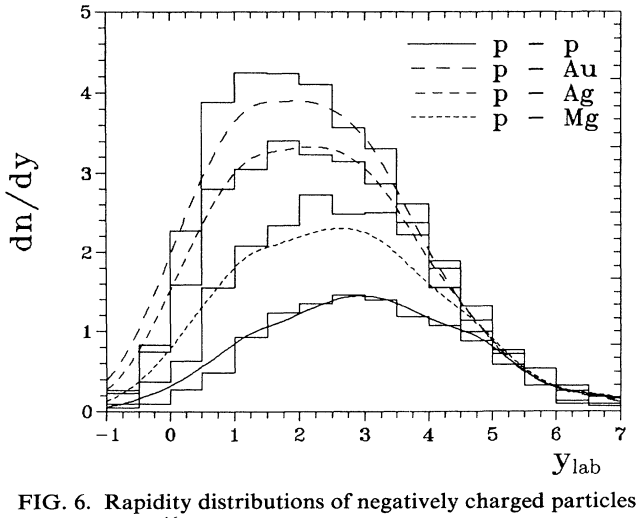

FIG. 6. Rapidity distributions of negatively charged particles from the central ^{16}O-Au collisions at 200 GeV/nucleon calculated in our parametrization (curve) in the comparison with the data (histogram).

teractions of each type in nucleus-nucleus collisions we use the Glauber-type calculation described in the previous section.

The results of the comparison of our parametrization predictions with the data are presented in Fig. 6. The data are taken from Ref. [10] at the laboratory energy 200 GeV/nucleon ^{16}O with Au central collisions. We have corrected our probabilities of internucleus interaction numbers to get approximately the same "centralities" ($\sigma \sim 50$ mb) as reported in Ref. [10].

The obtained distribution is a little wider than the experimental histogram. It can be evidence of the narrowing of the additional chain product distribution with an increase of the number of interactions ν. Here we assume a constant shape as it has been found for proton-nucleus interactions, for which ν is much smaller. To obtain a definite answer to the question how this shape should be changed, more data are needed.

V. SUMMARY AND DISCUSSION

The dual parton model and other models based on "first principles" (mainly the hadron structure and fragmentation functions measured in leptonic processes as well as some arguments based, more or less, on theory and confirmed empirically) describe well some characteristics of multiparticle production in hadronic interactions. Yet there are observed some discrepancies with experiments, even for rapidity distributions (cf., for example, Refs. [4,7]). It is due to the complexity of soft hadronic production processes.

In the present paper we propose the semiempirical parametrization of the rapidity distributions in soft multiparticle production processes. Generally, it is based on the dual parton model picture of hadron interactions. The shape of the rapidity distribution of individual chain products is found and parametrized for a very accurate set of data from the NA35 experiment.

We have also found the natural way to extrapolate the hadron-proton parametrization to hadron-nucleus and nucleus-nucleus interactions. The commonly used optical model of the nucleus is adopted. It is shown that within the two-chain model the self-consistent and accurate description of multiparticle production processes can be achieved from hadron-hadron to nucleus-nucleus interactions at about $\sqrt{s} \sim 20$ GeV.

[1] A. Capella, U. Sukhatme, Chung-I Tan, and J. Tran Thanh Van, Phys. Lett. **81B**, 68 (1979).

[2] B. Anderson *et al.*, Phys. Rev. C **97**, 31 (1983); T. Sjöstrand, Comput. Phys. Commun. **27**, 243 (1982); B. Anderson, G. Gustafson, and B. Nilsson-Almqvist, "A high energy string dynamics model for hadronic interaction," Lund Report No. Lu-TP-87-6, 1987 (unpublished); X. Cai, W. Chao, T. Meng, and C. Huang, Phys. Rev. D **33**, 1287 (1986); K. Chou, L. Liu, and T. Meng, *ibid.* **28**, 1080 (1983); R. C. Hwa and J. Pan, *ibid.* **45**, 106 (1992); A. Bialas, W. Czyż, and W. Furmański, Acta Phys. Pol. B **8**, 585 (1977); A. Białas and E. Białas, Phys. Rev. D **20**, 2854 (1979).

[3] A. Capella, J. A. Casado, C. Pajares, A. Ramello, and J. Tran Tranh Van, Z. Phys. C **33**, 541 (1987).

[4] M. Adamus *et al.*, Z. Phys. C **39**, 311 (1988).

[5] M. Adamus *et al.*, Z. Phys. C **32**, 475 (1986).

[6] A. Klar and J. Hüfner, Phys. Rev. D **31**, 491 (1985).

[7] N. M. Agababyan *et al.*, Z. Phys. C **50**, 361 (1991).

[8] D. M. Brick *et al.*, Phys. Rev. D **41**, 765 (1990).

[9] J. Engler, T. K. Gaisser, P. Lipari, and T. Stanev, in *Proceedings of the 22nd International Cosmic Ray Conference,* Dublin, Ireland, 1991, edited by M. Cawley *et al.* (Dublin Institute for Advanced Studies, Dublin, 1992), Vol. 4, p. 1.

[10] A. Bamberger *et al.*, Phys. Lett. B **203**, 320 (1988).